Crystal Structures and Melting Points of Unsaturated Triacylglycerols in the β Phase

S. de Jong, T.C. van Soest and **M.A. van Schaick**
Unilever Research Laboratorium Vlaardingen, P.O. Box 114, 3130 AC Vlaardingen, The Netherlands

The β-phase crystal structures of unsaturated triacylglycerols (TAGs) have been analyzed. Long spacings and melting points of monounsaturated TAGs such as *16 · O · 16* and *16 · O · 18* indicate a β-3C packing mode with a methyl terrace that differs from that of the saturated β-3 TAGs. In addition to the hydrocarbon chain subcell packing and the methyl terrace structure, the conformation of the oleoyl chain also has to be considered. This conformation is analyzed in connection with the symmetry relation between the two half-layers on either side of the plane through the double bonds. Geometric analysis shows four possibilities, which have been explored further by means of energy minimization computations. In these calculations the structure of the oleoyl chain, in its crystalline environment, has been optimized while taking all relevant intramolecular and intermolecular forces into account. Though the calculations reveal relatively small energy differences between the four possibilities, the most likely structure can still be identified. On the basis of the results obtained for the monounsaturated TAGs, proposals for the crystal structures of diunsaturated (*e.g., O · 18 · O*) and triunsaturated (*e.g., O · O · O*) TAGs are briefly outlined.

KEY WORDS: **β-Phase, crystal structure, energy calculation, polymorphism, triacylglycerols.**

The crystal structures of β-phase saturated triacylglycerols (TAGs) are now know in sufficient detail, either from single crystal X-ray diffraction analysis (1-4) or from model building studies (5,6). In this paper we extend our modeling studies to the crystal structures and melting points of unsaturated TAGs in the β modification. The unsaturated TAGs are of particular interest because they are major constituents of cocoa butter and confectionery fats, and also because they give rise to undesirable (re-)crystallization phenomena in palm oil products.

Throughout this paper the term "unsaturated" will be used in the restricted sense of "*cis*-unsaturated". With regard to solid-state properties, *trans*-unsaturated fatty acids behave rather like the saturated fatty acids and, hence, TAGs with such acyl chain have already been dealt with in our earlier work (5).

If we disregard the exact chemical structure of an acyl chain, apart from the distinction of saturated (*S*) as opposed to unsaturated (*U*), then the unsaturated TAGs may be divided into five classes—*S · U · S*, *U · S · S*, *U · S · U*, *U · U · S* and *U · U · U*. The stable form of TAGs belonging to the symmetrical classes *S · U · S*, *U · S · U* and *U · U · U* is β, whereas TAGs from the asymmetrical classes *U · S · S* and *U · U · S* do not occur in this β form. Hence, in this work, which concerns the β phase, we deal exclusively with the *S · U · S*-, *U · S · U*- and *U · U · U*-type TAGs. As before (5,6), the saturated fatty acids in a TAG will be denoted by the number of carbon atoms in the chain, and *p*, *g* and *r* represent chain 1, 2 and 3, respectively. The unsaturated acids will be denoted by *O* for oleic acid [(*Z*)-9-octadecenoic acid] and *Er* for erucic acid [(*Z*)-13-docosenoic acid].

Much of the work described in this paper concerns the crystal structures of the monounsaturated TAGs *p · O · r*. From the analysis of these TAGs, the main features of the crystal structures of the remaining *O · q · O* and *U · U · U* TAGs may be deduced in a fairly straightforward manner. It should be emphasized, however, that in these two cases the experimental evidence available for checking the proposed structures is particularly limited.

THE β PHASE OF MONOUNSATURATED TRIACYLGLYCEROLS

Molecular structure. We have already noted that only TAGs from the symmetrical classes *S · U · S*, *U · S · U* and *U · U · U* occur in the β crystal modification. Apparently, it is a prerequisite for the β form that the two outer chains are of like character. This is consistent with the adjacent packing of chains 1 and 3 observed in the β phase of saturated TAGs. Therefore, we assume that the molecular structure is very similar to that of the saturated TAGs in the β-2 and β-3 phases. The one essential difference between the saturated and the unsaturated TAGs obviously is that the geometry of the unsaturated chain will not be linear or, more correctly, zigzag, but rather bent or kinked.

Any chain conformation can best be described in terms of the torsion angles φ about the individual carbon-carbon bonds. Unsaturated chains show three types of carbon-carbon bonds, *viz.*, -CH_2-CH_2-, -CH_2-CH= and -CH=CH-. The first type usually adopts the *trans*- (or *anti*-) configuration ($\varphi \approx 180°$), especially when long chains in the solid state are concerned. The alternative, but less likely possibility, is that of a *gauche*-configuration ($\varphi \approx \pm 60°$). The torsion angle of the *cis* double bond is, by definition, zero, i.e., $\varphi \approx 0°$.

There is ample evidence that the C-CH_2-CH=C fragment differs from the C-CH_2-CH_2-C fragment with respect to its conformational behavior. This has been demonstrated clearly, for example, by the data we obtained from a literature search of the torsion angles of 350 C-C-C=C fragments from single crystal X-ray analyses of about 140 compounds, each containing this fragment (Fig. 1). The stable conformation are *skew* ($\varphi \approx \pm 120°$) and *cis* (or *syn*, $\varphi \approx 0°$), rather than *trans* or *gauche*. When the geometry of the double bond itself is already *cis* (Fig. 1B), as in oleic acid, the configuration around the single bond adjacent to the *cis* double bond can only be *skew*.

The conformation of the entire oleoyl chain now can be given in terms of the above-mentioned torsion angles using the following code: *c* for *cis* (0°), *g* for *gauche*$^+$ (60°), *s* for *skew*$^+$ (120°), *t* for *trans* (180°), $\bar{s}$ for *skew*$^-$ (240°), $\bar{g}$ for *gauche*$^-$ (300°) and *C* for the *cis* double bond.

To whom correspondence should be addressed: S. de Jong, Unilever Research Laboratorium Vlaardingen, Olivier van Noortlaan 120, 3133 AT Vlaardingen, The Netherlands.

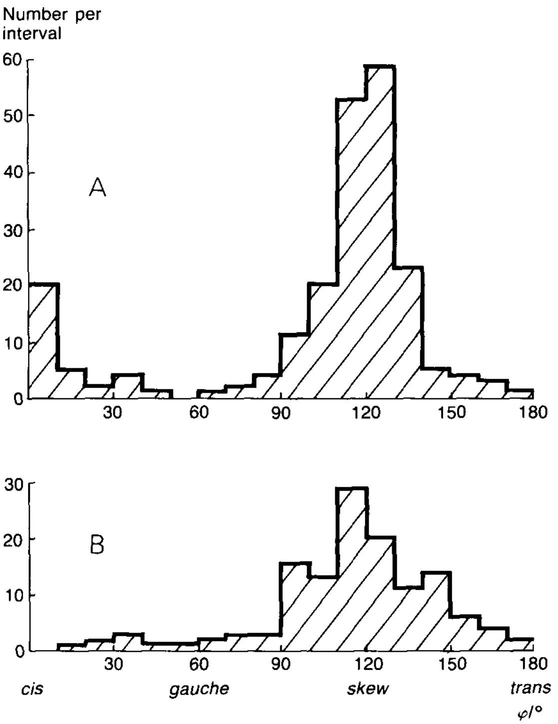

FIG. 1. Distribution of torsion angles, φ, in C=C fragments. A, X=H; B, X≠H.
X C-C

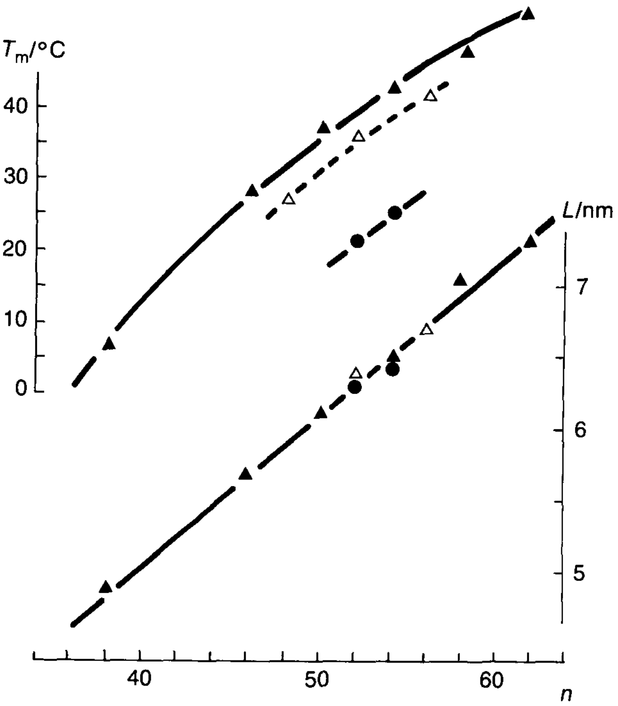

FIG. 3. Long spacings (*L*) and melting points (T_m) of β-3 phase unsaturated triacyglycerols as a function of the total number of acyl chain carbon atoms (*n*). ▲, *p · O · p*; △, *p · O · p+2*; and ●, *O · q · O*.

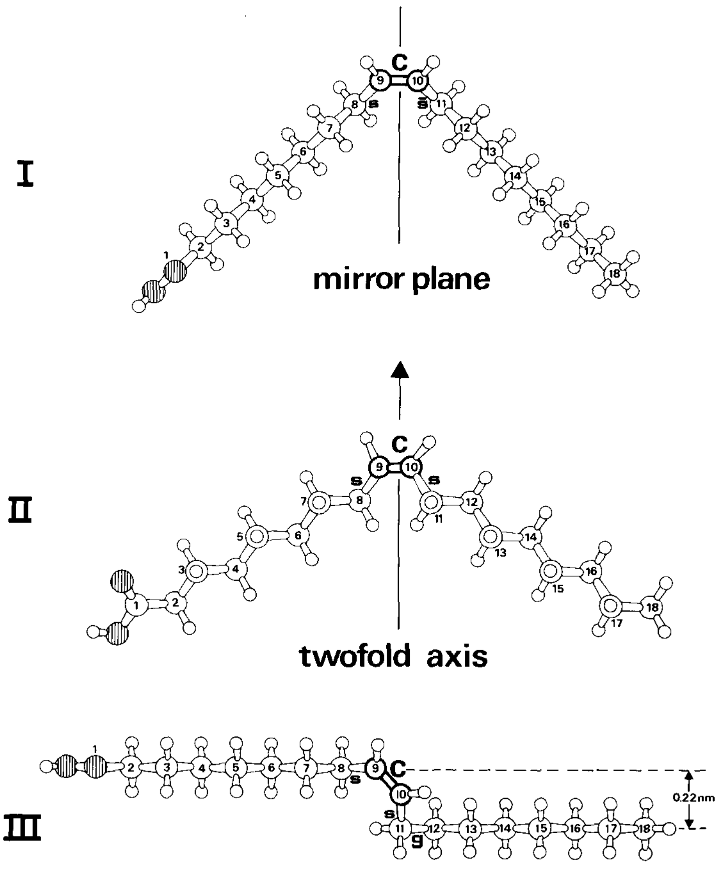

FIG. 2. Conformations of oleic acid: (I) . . . *sC*$\bar{s}$ . . .; (II) . . . *sCs* . . .; and (III) . . . *sCsg* . . ..

TABLE 1

Experimental Long Spacing *(L)* and Melting Point *(T_m)* Data of Unsaturated Triacylglycerols in the β Phase

Triacylglycerol		*n*	*L*/nm	Refs.	T_m/°C	Refs.
p · O · p	(symmetric monounsaturated TAGs)					
	10 · O · 10	38	4.88	9	6.2	9
	14 · O · 14	46	5.67	10	28.5	10
	16 · O · 16	50	6.1, 6.07, 6.09	9, 10, 11	35.2, 37.5, 38.3	9, 10, 11
			6.04, 6.05, 6.3	11, 12, 13	36, 38, 37.2	11, 12, 13
			6.16, 6.10	14, 15	35.5, 36.7	14, 15
	18 · O · 18	54	6.5, 6.41, 6.48	9, 16, 10	43.0, 42.0, 43.5	9, 16, 10
			6.5, 6.47, 6.50	17, 18, 15	41.7, 43.5, 43.0	17, 18, 15
	20 · O · 20	58	7.07	19	48.3	19
	22 · O · 22	62	7.36	19	53.3	19
p · O · p+2	(asymmetric monounsaturated TAGs)					
	14 · O · 16	48	—	—	27	
	16 · O · 18	52	6.31, 6.41, 6.37	20, 21, 17	38, 37.7, 35.7	20, 21, 17
			6.26, 6.43, 6.40	22, 23, 18	35.5, 35.0	23, 18
	18 · O · 20	56	6.7	[a]	41.5	[a]
O · q · O	(diunsaturated TAGs)					
	O · 16 · O	52	6.30, 6.35	24, [a]	21.0	24
	O · 18 · O	54	6.44, 6.50	24, 25	25.4, 25, 24.5	24, 25, [a]
U · U · U	monoacid triunsaturated TAGs)					
	O · O · O	54	4.33, 4.25	26, 25	5.5, 5	26, 25
	Er · Er · Er	66	5.13, 5.11	27, 28	31.5, 30	27, 29

[a] This work.

Assuming that the saturated parts of the oleoyl chain are in the fully extended all-*trans* configuration we derive two essentially different conformations: . . . *ttsC*$\bar{s}$*tt* . . . (I) and . . . *ttsCstt* . . . (II). These conformations are displayed in Figure 2. A salient feature of such conformations is the pseudo-symmetric relationship between both chain halves, namely a reflection for I and a two-fold rotation for II. The third conformation shown in Figure 2, . . . *ttsCsgt* . . . (III), is intriguing because it has an overall straight configuration.

At this stage of the analysis it is not possible to make a decisive choice between the three conformations. However, an indication in favor of conformation I comes from the crystal structure of oleic acid (7), which has this very conformation. An argument against the third conformation is that it involves one, energetically less favorable, *gauche* torsion angle. It does occur, however, in the crystal structure of cholesteryl palmitoleate (8). Disregarding the precise conformation of the oleoyl chain, however, we shall first consider the lateral packing of the molecules in the β crystalline phase.

Lateral packing. All available long spacing and melting point data for the unsaturated β-phase TAGs have been collected in Table 1. In Figure 3 these data have been plotted as a function of the total number of chain carbon atoms, $n \equiv p+q+r$). A β-3 packing mode of the molecules is immediately apparent from the high values of the long spacings. A β-3 structure is perfectly logical because it allows side-by-side packing of the unsaturated chains. These unsaturated chains are sandwiched between layers of saturated chains packed laterally. In the β-2 packing mode the unsaturated chains would have had to be packed in-between the saturated chains.

For a more detailed discussion of the lateral packing we can benefit from our previous analysis of the β-3 phase of saturated TAGs (6). Starting from the assumption that the $T_{//}$ subcell hydrocarbon chain packing is responsible for the underlying structure of each β phase, geometric analysis of the packing and subsequent lattice energy calculations indicated that the expressions for the unit cell axes **a** and **b**, in terms of the subcell axes $\mathbf{a}_s$, $\mathbf{b}_s$ and $\mathbf{c}_s$, are:

$$\mathbf{a} = 2\mathbf{a}_s + t\mathbf{c}_s \qquad [1]$$

and

$$\mathbf{b} = \mathbf{b}_s. \qquad [2]$$

It was also found that only two solutions were admissible, *viz.*, $t = 1$ and $t = -1$. The first solution, $t = 1$, (calculated $\tau = 67°$) applies to the saturated β-3 TAG systems. The alternative solution, $t = -1$ (calculated $\tau = 56°$), although theoretically quite feasible, had to be discarded for the saturated TAGs because, among other things, it disagreed with the observed value angle of tilt: $\tau = 66°$. For the present β-3 unsaturated TAGs, the least squares linear equation for the experimental long spacing (Fig. 3) is:

$$L = (n + 9.2) \cdot 0.103 \text{ nm} \qquad [3]$$

The standard errors are 2.0 for n_0 and 0.003 nm for the slope. The estimated value of 9.2 for n_0 is not significantly different from the values ($n_0 \approx 6$–7) found earlier for the saturated β-2 and β-3 TAGs (5,6). This is as expected because n_0 accounts for the space occupied by the non-subcell regions (glycerol group and methyl end groups) and probably does not depend much on the particular packing mode.

From the slope we obtain an angle of tilt $\tau = \sin^{-1}(0.103 \cdot 2/0.2545) = 54°$ with a standard error of 3^0. Hence, for the unsaturated TAGs, the solution $t = -1$ applies and, consequently, the **a** axis is given by:

$$\mathbf{a} = 2\mathbf{a}_s - \mathbf{c}_s. \qquad [4]$$

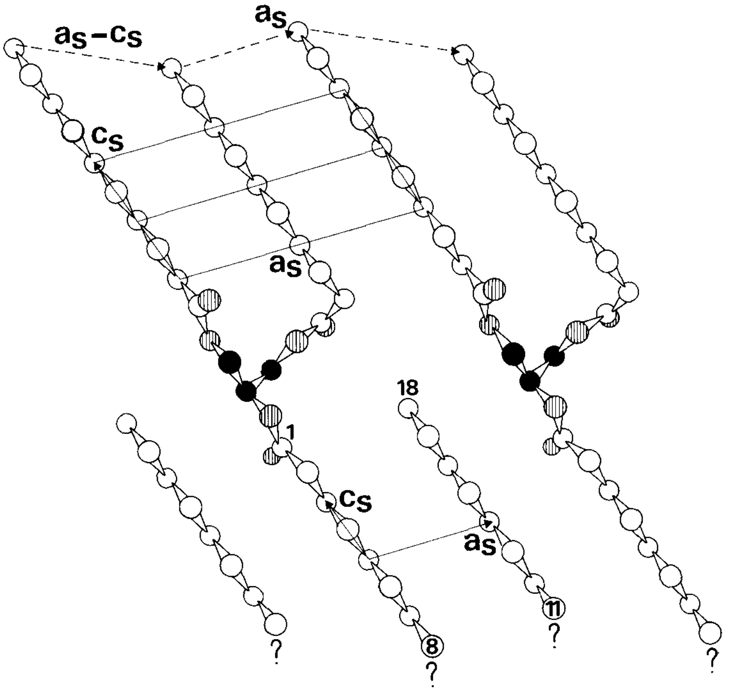

FIG. 4. Lateral arrangement of $p \cdot O \cdot p$ triacylglycerols (p=10), showing the subcell packing and the methyl terrace. Only half a layer is shown. Projection is on the a_sc_s-plane.

In Figure 4 this type of packing is displayed for a $p \cdot O \cdot p$ TAG. Only half a layer is shown since we do not yet know the structure of the oleoyl chain. The methyl terrace, with the terrace indices (−1,0), will be denoted henceforth as β-3*C* and should be distinguished from the β-3*A* (0.1) and β-3*B* (−1,2) terraces found for the saturated TAGs (6). A simple extension of chain 3 by two carbon atoms, transforming $p \cdot O \cdot p$ into $p \cdot O \cdot p{+}2$, leaves the methyl terrace essentially unaltered [(−1, 0) → (0, −1)].

So, the $p \cdot O \cdot p$ and $p \cdot O \cdot p{+}2$ TAGs share the same β-3*C* terrace. For entropy reasons (5,6), the melting point line of the asymmetric $p \cdot O \cdot p{+}2$ TAGs should then lie about 4°C beneath the one for the symmetric $p \cdot O \cdot p$ TAGs. This is indeed observed (Fig. 3). In sum, the combined evidence of long spacing data, melting points, geometric packing analysis and lattice energy calculations (6) leads unambiguously to the β-3*C* lateral packing given by Eqs. [2] and [4] and illustrated in Figure 4.

Assembly of the two half-layers. The next step is to "weld" the two half-layers together in such a manner as to give an acceptable conformation for the oleoyl chain and having no short nonbonded atom-atom contacts between neighboring oleoyl chains. We will assume that the two layer halves are related through a crystallographic symmetry element. Even if this assumption should not hold fully, the true structure, with two independent molecules in the asymmetric unit, probably departs only slightly from the more symmetric situation.

Geometric analysis. The (pseudo-) symmetry elements that may be conceived are a (glide-)reflection, a two-fold (screw-)rotation and an inversion. In principle, the oleoyl chain conformation (Fig. 2) should be compatible with this crystallographic symmetry. Hence, a mirror symmetry must be associated with conformation I, the rotation symmetry with conformation II and the inversion symmetry, giving rise to essentially straight oleoyl chains, with conformation III. The center of symmetry and the mirror (glide) plane parallel to the *ab* plane put no additional constraints upon the **a** and **b** axes, which have already been fully established (Eqs. [2] and [4]). The converse is true for rotation symmetry, because a two-fold axis in the *ab* plane implies the presence of a unique axis in this plane at right angles to the other unit cell axes. With the **a** and **b** axis given by Eqs. [4] and [2], respectively, it turns out that the **b** axis is almost perpendicular to the *ab* diagonal axis **a**′:

$$\mathbf{a}' \equiv \mathbf{a} + \mathbf{b} = 2\mathbf{a}_s + \mathbf{b}_s - \mathbf{c}_s. \qquad [5]$$

On the basis of the subcell dimensions given in our earlier work (5), the angle $\gamma' = 89.2°$. With a minor adaptation of the subcell γ_s angle, *viz.*, from 121° to 121.9°, an exact right angle for γ' is achieved. Consequently, the possibility of a two-fold (screw) axis, either parallel to **a**′ or to **b**, is real.

Altogether there are now four options for the symmetry operation transforming the two half-layers: i) a glide plane // *ab* with an *a*/2 glide; ii) a two-fold screw axis // **a**′; iii) a two-fold screw axis // **b**; and iv) the inversion symmetry. We have constructed computer models for each of these four structures. The two layer halves were placed around the symmetry element in such a way that carbon atoms C8 and C11 of the oleoyl chain are at a distance (0.315 nm) dictated by the rigid geometry of the *cis* C8-C9=C10-C11 fragment. Subsequently, the coordinates of the double bond atoms C9 and C10 are generated in 36 different ways, corresponding to a full revolution of the C8-C9=C10-C11 fragment, in steps of 10°, around the C8 · · · C11 axis. For each of the ensuing structures the torsion angles around the bonds C7-C8, C8-C9, C10-C11 and C11-C12 and the bond angles C7-C8-C9 and C10-C11-C12 were computed. Surprisingly, all four symmetries gave acceptable conformations, *i.e.*, with the torsion

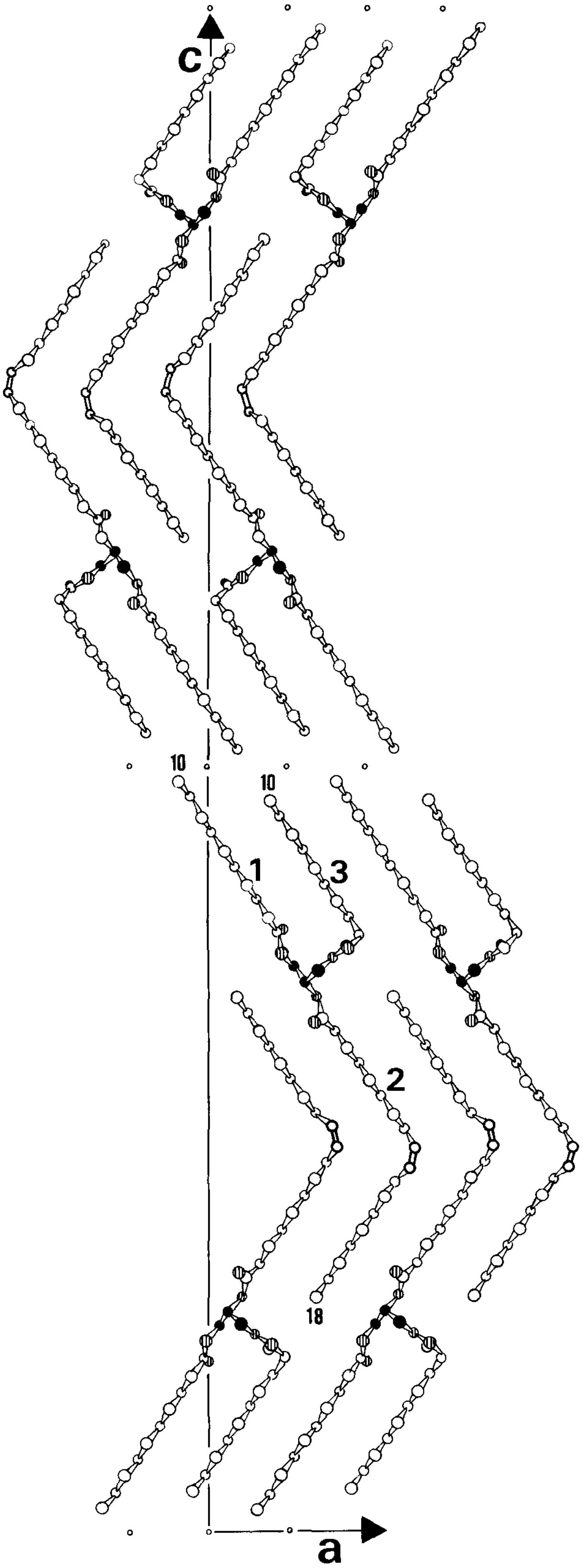

FIG. 5. Proposed crystal structure for β-3*C* monounsaturated *p* · *O* · *p* triacylglycerols (p=10). Space group $P2_1/a$ assumed.

halves we may conceive several symmetry elements relating the layers, *viz.* a center of symmetry, (glide-)reflections or two-fold (screw-)axes. We have not investigated the stacking of the layers in any further detail because it is of less importance than the structure of the layer itself. Moreover, there would be no way to check the theoretical results with the experimental data. In Figure 5 the structure of *16* · *O* · *16* is illustrated, assuming a glide plane to be present at the double bonds and inversion centers between the methyl groups. We have suggested earlier (33) that the phase transformation V→VI in cocoa butter (18,34), which is responsible for the formation of "bloom" on chocolate, involves a change of the layer stacking, giving a higher crystal symmetry and resulting in a simpler powder diffraction pattern. Also, the subtle difference between the so-called β_1 and β_2 forms observed by Sato *et al.* (15) may lie in a different stacking of the layers. However, these are mere speculations, which probably can be settled only by single crystal X-ray diffraction analyses.

THE β PHASE OF SYMMETRIC DIUNSATURATED TRIACYLGLYCEROLS

The long spacings of the *O* · *q* · *O* TAGs, plotted as a function of *n*, coincide with those of the monounsaturated *p* · *O* · *r* TAGs (Fig. 3). As a result, the lateral packing and the methyl terrace are probably identical. An obvious solution to the crystal structure is therefore a β-3*C* structure with the unsaturated chains at the outsides and the saturated chains at the inside of the layer. The symmetry element at the center of the layer can be an inversion only, since a two-fold (screw-)axis or a (glide-)reflection would lead to non-straight saturated chains.

There can be no true symmetry at the planes through the double bonds, but there may be a local pseudosymmetry relation between the oleoyl chain halves. All four possibilities proposed in the foregoing section may be considered again. Since the methyl terrace is exactly the same as that for the monounsaturated TAGs, the same considerations regarding the layer stacking apply here. In Figure 6 the simplest possible structure is shown with a center of symmetry between the layers and a pseudomirror plane at the double bonds.

THE β PHASE OF TRIUNSATURATED TRIACYLGLYCEROLS

The low values for the long spacing of β-phase *O* · *O* · *O* and *Er* · *Er* · *Er* (trierucin) (Table 1) show that these triunsaturated TAGs crystallize in a β-2 modification. Since there is no distinction between chains 1 and 3 on the one hand, and chain 2 on the other, there is no "advantage" for the β-3 packing mode. Compared to their saturated analogs (1), the long spacings lie between those of the β-2*A* and the β-2*E* submodification, though somewhat closer to the former. A satisfactory model for the *A*-type structure is shown in Figure 7. However, we have not pursued the analysis beyond this stage of explorative model building since the crystal structures of these low-melting compounds are of less practical interest.

DISCUSSION

The work described in this report forms the first investigation of the crystal structures of unsaturated TAGs at the atomic level of detail. Previously, more schematic proposals for these structures have been put forward angles and bond angles not too far from their favored values, demonstrating the feasiblity of these four different structures.

Energy minimization calculations. A more comprehensive analysis, however, should take into account all intra- and intermolecular interactions and thus establish the minimum energy structure. This we have done by means of the *QCFF/MCA* program package (30,31), which allows optimization of all atomic positions of a molecule in a crystalline environment. The force field given (30) includes all relevant conformational and packing potential functions: bond stretching (U_{str}), angle bending (U_{bend}), torsion (U_{tors}) and intramolecular (U_{nonb}), as well as intermolecular (U_{cryst}) non-bonded interactions.

The calculation of a complete TAG molecule, having 100-200 atoms, however, would involve a prohibitive amount of computing time. Furthermore, we are interested only in the optimum conformation and packing near the double bonds of the oleoyl chains. Thus, for our purpose, it is sufficient to consider only part of the oleoyl chain. In fact, we have used (*Z*)-5-nonene as a model for the C5-C13 fragment of oleic acid.

The "best" structures derived from the earlier computer modeling exercise served as the starting points for the *QCFF/MCA* calculations. In order to ensure a smooth transition from the double bond region C7-C12 to the subcell regions C1-C8 and C11-C18, both propyl ends of the nonene molecule were kept in a position prescribed by the subcell packing. This was achieved by judiciously chosen penalty functions, which were added to the program. By doing so, six torsion angles, five bond angles and four bond lengths of the carbon chains remained to be optimized. The final results of these calculations are given in Table 2.

The optimized structures of the oleoyl chain are clearly interpretable in terms of the idealized stable conformations. Their energy differences, however, are too small to warrant a preference for any of these structures. This is because the accuracy of the calculations is not high enough, the calculated energy differences being only a few kJ/mol. We must also take into account kinetic factors operating during the crystallization process. Hence, even if the energy differences are real, this does not automatically imply that the low-energy structure, i), is the one formed in practice.

It should be recalled, however, that the conformation of the oleoyl chain in structure i) very closely resembles the one found in the crystal structure of oleic acid (last column of Table 2). Furthermore, an argument against the ii) and iii) structures is that the symmetry-related molecules inside a layer are not optical antipodes. Then, for the racemic $p \cdot O \cdot p{+}2$ TAGs the implication is that the stereoisomers are packed alternately in separate layers. Depending on the mechanism of crystal growth, this may be kinetically unfavorable, and a structure such as i) or iv), which have both *D* and *L* molecules inside one layer, may develop more readily. In this connection it is also interesting to observe that chiral $16 \cdot O \cdot 18$ does not crystallize in a β phase (22). Should it have done so, then structures i) and iv) would have had to be excluded. If the structure is ii) or iii), then it is hard to understand why the optically active $16 \cdot O \cdot 18$ does not crystallize in the β modification. All these considerations lead to the conclusion that the most probable structure is i). An attempt to arrive at a decision by comparing the experimental powder diffraction diagrams with calculated diagrams (32) based on the refined theoretical structures has been unsuccessful.

Layer stacking. Just as with the packing of the layer

TABLE 2

Optimized Structures and Energies of the Oleoyl Chains in the Four Different Lateral Packing Modes of β-3 Unsaturated Triacylglycerols

Parameter		Structure				Oleic
		i)	ii)	iii)	iv)	acid[a]
Bond angle/°	θ_7	111.6	109.4	114.4	115.1	111.0
	θ_8	108.6	110.3	109.4	110.3	105.8
	θ_9	126.6	126.5	126.6	127.4	125.8
	θ_{10}	127.3	127.7	127.0	126.4	125.6
	θ_{11}	108.5	109.4	109.9	114.3	107.4
Torsion angle.°	$\varphi_{6\text{-}7}$	185	188	184	183	180
	$\varphi_{7\text{-}8}$	180	175	84	66	176
	$\varphi_{8\text{-}9}$	124	121	126	131	132
	$\varphi_{9\text{-}10}$	0	-4	2	-4	-2
	$\varphi_{10\text{-}11}$	-138	118	-137	123	-128
	$\varphi_{11\text{-}12}$	-162	162	160	173	-171
Relative energy/ (kJ mol^{-1})	U_{str}	0.0	-0.4	-0.6	-1.5	—
	U_{bend}	0.0	1,8	1,7	5.5	—
	U_{tors}	0.0	-1.3	2.8	-1.5	—
	U_{nonb}	0.0	-0.9	1.1	1.5	—
	U_{cryst}	0.0	2.3	1.2	3.6	—
	U_{total}	0.0	1.5	6.1	8.0	—
Symmetry		**a** glide	$2_1//\mathbf{a}'$	$2_1//\mathbf{b}$	$\bar{1}$	
Conformation		. $ttsC\bar{s}t$.	. $ttsCst$.	. $tgsC\bar{s}t$.	. $tqCst$.	. $ttsC\bar{s}t$.

[a] Ref. 7.

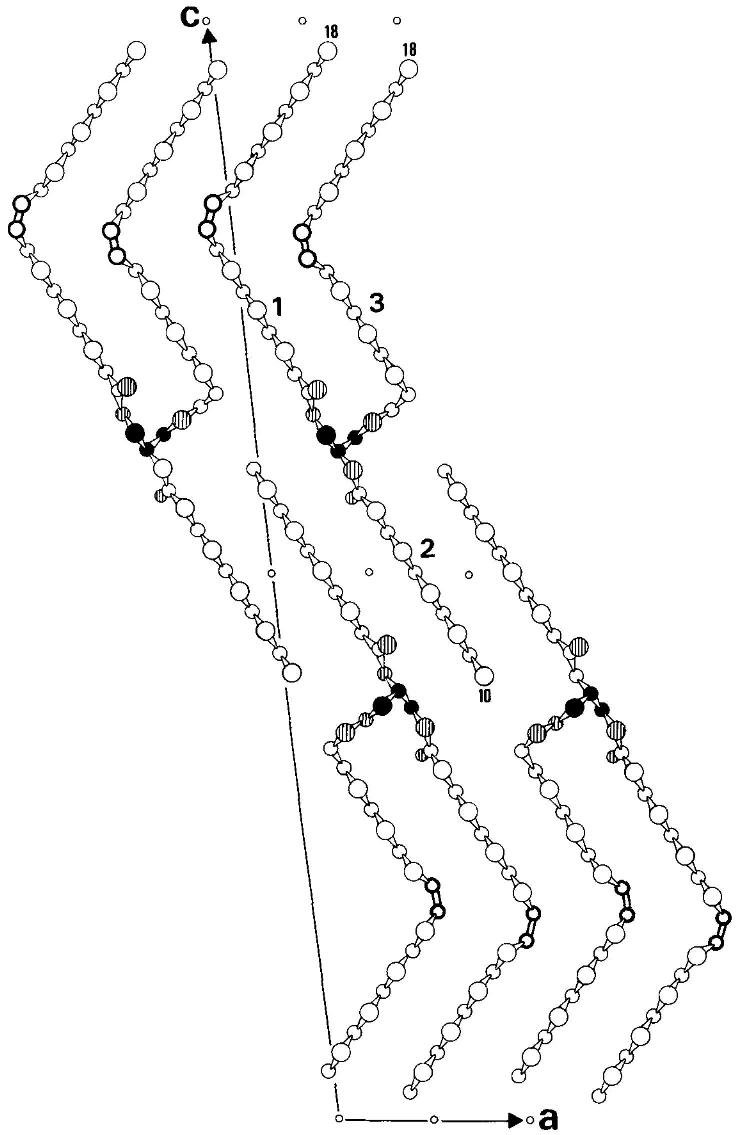

FIG. 6. Proposed crystal structure for β-3*C* diunsaturated *O* · *p* · *O* triacylglycerols (*p*=10). *P*$\bar{1}$ symmetry assumed.

(34–36). For example, the β-3 packing mode, as opposed to the common β-2 packing, was immediately recognized by the first workers who used X-ray powder diffraction as a tool to study the polymorphism of unsaturated TAGs.

Larsson (35) considered the β-3 crystal structure of *18* · *O* · *18* in some more detail and arrived at a rough structure resembling our model (Fig. 5). However, both the molecular structure and the lateral packing ($O'_{//}$ subcell) of the oleoyl chains were adopted from the crystal structure of oleic acid (7). For the saturated chains the $T_{//}$ subcell packing was assumed. Until now, however, no crystal structure of a long-chain compound is known that incorporates different types of hydrocarbon chain packing. A theoretical argument opposing the idea of accommodating two different subcells in a common crystal structure is that it is not possible to find short unit cell axes that can be expressed as simple linear combinations of the $T_{//}$ subcell axes and the $O'_{//}$ subcell axes at the same time. Furthermore, the powder diffraction patterns do not provide conclusive evidence that the $O'_{//}$ subcell prevails. For these various reasons we consider, with respect to the lateral arrangement of the oleoyl chains, the proposed structure not to be entirely correct.

A very detailed structure has been proposed for the β phase of *16* · *O* · *18* as a model for the stable modification of cocoa butter (34). The proposal is based on rather poor evidence—the chain packing has not been considered, the angle of tilt used is too high, and the conformation of the oleoyl chain is deduced from a consideration of the β-phase long spacing.

In our work several packing modes have been shown to be theoretically feasible for the monounsaturated TAGs *p* · *O* · *r*. In practice this may well be reflected by the complex phase behavior of cocoa butter, which has two β-3-like phases (12,34). We have also shown the close similarity of the crystal structures of *16* · *O* · *16*, *16* · *O* · *18*

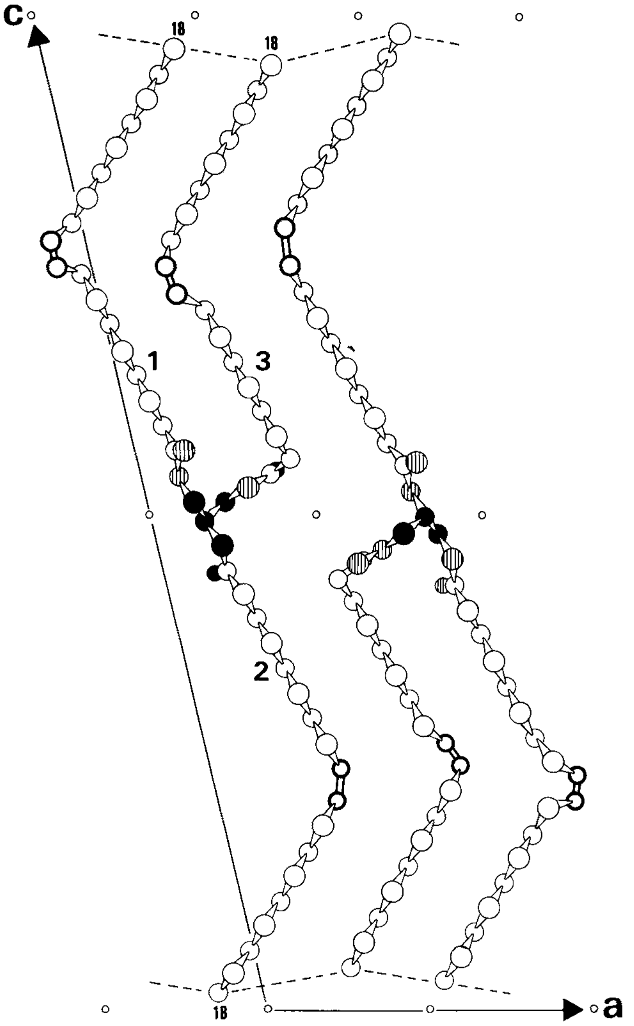

FIG. 7. Proposal for the β-2*A* crystal structure of triunsaturated glyceroltrioleate (*O* · *O* · *O*).

and *18* · *O* · *18*, which may explain the high extent to which each of these compounds can dissolve in the solid state of the others (12,37,38).

Reviewing our analyses of the structures of β-2 saturated TAGs (5), of β-3 saturated TAGs (6) and the present unsaturated TAGs, we note that the experimental data have become increasingly sparse, the analyses relying more and more on theoretical calculations and the results becoming less and less conclusive. We believe that with the present work the utmost has been done to clarify the crystal structures of β-phase TAGs on the basis of available experimental data. Further progress in the field can only be achieved by single-crystal structure analyses. This is particularly true of the β' modification, where a structure that has been completely solved could serve as a starting point from which to develop alternative β' crystal structures. This could be done by using a similar approach as our model building studies of the various β phase crystal structures. Such an approach may produce a survey of a great variety of structures, determine their common features and uncover their essential differences.

REFERENCES

1. Larsson, K., *Arkiv Kemi 23*:1 (1964).
2. Jensen, L.H., and A.J. Mabis, *Acta Crystallogr. 21*:770 (1966).
3. Doyne, T.H., and J.T. Gordon, *J. Am. Oil Chem. Soc. 45*:333 (1968).
4. Gibon, V., P. Blanpain, B. Norberg and F. Durant, *Bull. Soc. Chim. Belg. 93*:27 (1984).
5. de Jong, S., and T.C. van Soest, *Acta Crystallogr. B. 34*:1570 (1978).
6. van Soest, T.C., S. de Jong and E.C. Roijers, *J. Am. Oil Chem. Soc. 67*:415 (1990).
7. Abrahamsson, S., and I. Ryderstedt-Nahringbauer, *Acta Crystallogr. 15*:1261 (1962).
8. Craven, B.M., and P. Sawzik, *J. Lipid Res. 25*:857 (1984).
9. Filer, L.J., S.S. Sidhu, B.F. Daubert and H.E. Longenecker, *J. Am. Chem. Soc. 68*:167 (1946).
10. Malkin, T., and B.R. Wilson, *J. Chem. Soc.*:369 (1949).
11. Lutton, E.S., and F.L. Jackson, *J. Am. Chem. Soc. 72*:3254 (1950).
12. Goto, M., *Yukagaku 19*:583 (1970).
13. Lovegren, N.V., M.S. Gray and R.O. Feuge, *J. Am. Oil Chem. Soc. 48*:116 (1971).
14. Gibon, V., F. Durant and Cl. Deroanne, *Ibid. 63*:1047 (1986).
15. Sato, K., T. Arishima, Z.H. Wang, K. Ojima, N. Sagi and H. Mori, *Ibid. 66*:664 (1989).
16. Lutton, E.S., *J. Am. Chem. Soc. 68*:676 (1946).
17. Lavery, H., *J. Am. Oil Chem. Soc. 35*:418 (1958).
18. Wille, R.L., and E.S. Lutton, *Ibid. 43*:491 (1966).
19. Wang, Z.H., K. Sato, N. Sagi, T. Izumi and H. Mori, *J. Japan Oil Chem. Soc. 36*:671 (1987).
20. Lutton, E.S., *J. Am. Chem. Soc. 73*:5595 (1951).
21. Chapman, D., A. Crossley and A.C. Davies, *J. Chem. Soc.*, 1502 (1957).
22. Schlenk, W., *J. Am. Oil Chem. Soc. 42*:945 (1965).
23. Lutton, E.S., *Ibid. 34*:521 (1957).
24. Lutton, E.S., *Ibid. 43*:509 (1966).
25. Kodali, D.R., D. Atkinson, T.G. Redgrave and D.M. Small, *J. Lipid Res. 28*:403 (1987).
26. Ferguson, R.H., and E.S. Lutton, *J. Am. Chem. Soc. 69*:1445 (1947).
27. Hilditch, T.P., and M.L. Meara, *J. Chem. Soc.*, 1608 (1938).
28. Carter, M.G.R., and T. Malkin, *Ibid.*:554 (1947).
29. Carter, M.G.R., and T. Malkin, *Ibid.*:1518 (1939).
30. Warshel, A., and M.A. Karplus, *J. Am. Chem. Soc. 94*:5612 (1972).
31. Huler, E., and A. Warshel, *Acta Crystallogr. B. 30*:1822 (1974).
32. Clark, C.M., D.K. Smith and G.G. Johnson, *A Fortran IV Program for Calculating X-Ray Powder Diffraction Patterns-Version 5*, The Pennsylvania State University, Department of Geosciences, Pennsylvania, 1973.
33. van Soest, T.C., and S. de Jong, *J. Am. Oil Chem. Soc. 54*:158 (1977).
34. Witzel, H., and K. Becker, *Fette Seifen Anstrichm. 71*:507 (1969).
35. Larsson, K., *Ibid. 74*:136 (1972).
36. Hagemann, J.W., W.H. Tallent and K.E. Kolb, *J. Am. Oil Chem. Soc. 49*:118 (1972).
37. Rossell, J.B., *Adv. Lipid Res. 5*:353 (1967).
38. Rossell, J.B., *Chem. Ind. (London)*, 832 (1973).

[Received January 21, 1991; accepted February 22, 1991]